ORDEM DOS ENGENHEIROS
INFORMAÇÃO GEOESPACIAL PARA AS GERAÇÕES FUTURAS
OPORTUNIDADES E DESAFIOS
VIII CNCG
CONFERÊNCIA NACIONAL DE CARTOGRAFIA E GEODESIA
29 e 30 de outubro de 2015

Application of an operational model to forecast near-shore circulation: the case study of S. Jacinto beach

*Diogo MENDES[1], José PAULO PINTO[1] e António JORGE DA SILVA[1]

[1] Instituto Hidrográfico, Rua das Trinas nº49 1249 - 093 Lisboa

(diogo.mendes@hidrografico.pt; paulo.pinto@hidrografico.pt; jorge.silva@hidrografico.pt)

Keywords: Near-shore circulation, Field data collecting, Numerical modelling, Operational forecasting system

Abstract: Near-shore areas constitute a significant part of the Portuguese economy. In these areas, several activities take place such as yachting, aquaculture and tourism. The wave climate in near-shore zones can be very energetic, thereby representing a large source of risks such as coastal erosion and storm surges. For this reason, the development of an operational model able to forecast the near-shore circulation has become a key issue to ensure the sustainability of coastal environments. For such purpose, SMARTWAVE was developed and this study aims to apply it to a real coastal environment.

Recently, a field campaign was performed by the Portuguese Instituto Hidrográfico at S. Jacinto beach, NW Portugal. In this campaign, background current profile and wave parameters were obtained by an ADCP moored over 11 m depth and an array of eight pressure sensors was used to measure the wave shoaling, breaking, dissipation and set-up near the coastline. Topo-bathymetric data were also collected at the beach by a quad-bike and by a jet-ski, thereby assuring the good reproduction of the entire inter-tidal zone. Moreover, several drifters were launched in the area between the breaker zone and the coastline to obtain the pattern of the current field at the sea surface. Previous measurements were used to calibrate the empirical formulations (i.e. wave breaking). It is expected that this operational model will become a reliable tool to predict the circulation patterns in near-shore zones.

1. Introduction

The ability to predict waves and currents in coastal environments is a key issue for their sustainable management. Local authorities need this type of resources when developing coastal policies for commercial or navigation purposes. Coastal areas are located at the sea-land interface where several activities take place such as yachting, aquaculture and tourism. The many human interventions in these sites (i.e. buildings) increased the risks which they are subjected to, such as coastal erosion and storm surges. For that reason, the development of an operational model (SMARTWAVE) able to forecast the near-shore circulation becomes of utmost importance.

In near-shore areas, the morphological changes induced at the bottom by the complex interaction between waves and currents in the breaking zone can occur in time scales of weeks and months. Therefore, one of the limitations in these operational models is the lack of a good bathymetry near the coastline (Austin *et al*., 2012). Usually, the near-shore prediction models consist of a global (Tolman, 2002 and Chassignet *et al.*, 2007)), a regional (Booj *et al.*, 1999) and a near-shore model (Figure 1). Recently, the near-shore models become sophisticated and can now predict inundations due to storm surges (Lim *et al*., 2013). SMARTWAVE is our near-shore model and it aims to simulate the wave propagation and currents interactions from the coastal ocean to the coastline.

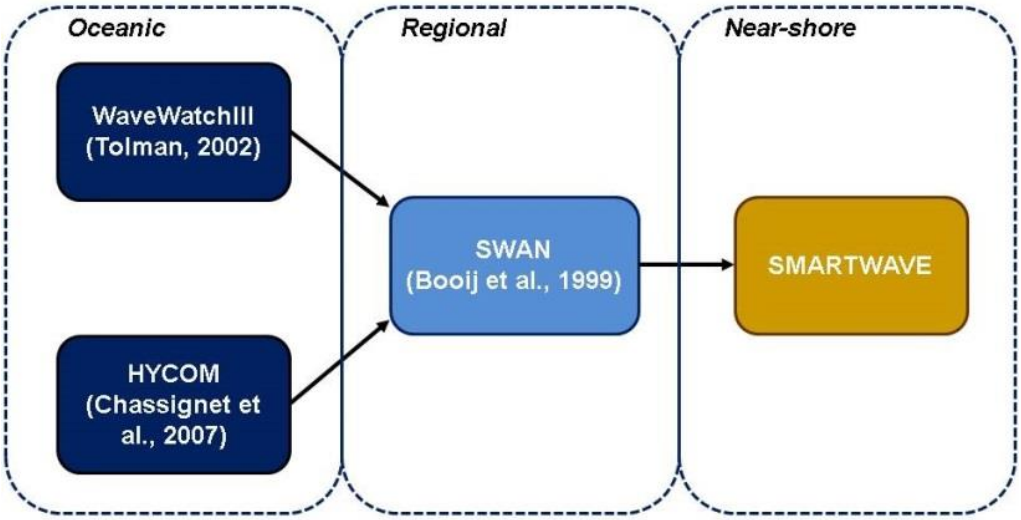

Figure 1 - Operational modelling system currently in development at Instituto Hidrográfico (IH) from oceanic to near-shore spatial scales

Several wave mechanisms must be accounted for in this operational model. The wave refraction due to bottom changes towards the coastline can induce changes in the wave celerity along a wave crest and, therefore, induce further changes in the wave direction. Near coastal structures built at the coast, such as jetties or breakwaters, wave diffraction plays a major role and significantly shifts the wave direction and amplitude. On the top of these, the most important wave dissipation mechanisms (breaking and bottom friction) must also be accounted for.

Previous authors had used the mild-slope equation or the Boussinesq equations to model previous energy dissipation mechanisms (Shi *et al*., 2012; Sharma *et al*., 2014). However, the computational cost is a requirement in these formulations since they need between eight and twelve grid nodes per wavelength to reach acceptable results (Dingemans, 1997). Therefore, the mild-slope equation was used with a smaller difference on the physical formulation in order to obtain acceptable results with only three to four grid nodes per wavelength.

Several laboratory or field tests were carried out in the last decades in order to verify the performance of wave models. Laboratory test cases are usually used to verify the wave diffraction and refraction (Berkhoff *et al*., 1982). Field tests are generally used to obtain current data and wave parameters offshore (Birkemeier *et al*., 1996). However, observational data measurements are not always available. For that reason, we decided to make a field campaign in a mild-slope beach in order to measure the wave propagation until the coastline and also the current field.

The objectives of this study were two-fold. Firstly, to examine the capability of obtaining data from the breaking zone. Secondly, to apply the wave model to S. Jacinto and compare its results with the measurements.

2. Field campaign

2.1 Brief characterization of S. Jacinto beach

S. Jacinto beach is located north of the Aveiro jetted inlet at the north-western Portuguese coast. Based on the Leixões wave buoy, the wave regime in S. Jacinto beach can be briefly characterized by a significant wave height (Hs) between 1.5 and 4 m, a wave peak period (Tp) between 10 and 16 s and a mean wave direction (Dir) confined to a sector between W and NW. The longshore sediment transport has a N-S direction mainly due to the wave direction. The last 36 years of tidal predictions for the entrance of the Aveiro inlet show a maximum high-water during spring tides of 3.76 m above the tidal reference (TR) and a minimum low-water during spring tides of 0.24 m (TR). The tidal regime can be characterized by a low meso-tidal coast with an average tidal amplitude of 2,0 m. In this type of coasts, the wave forcing usually shape the coastline leading to a complex system of sand cusps with rip currents as we observed during the field campaign (Figure 2).

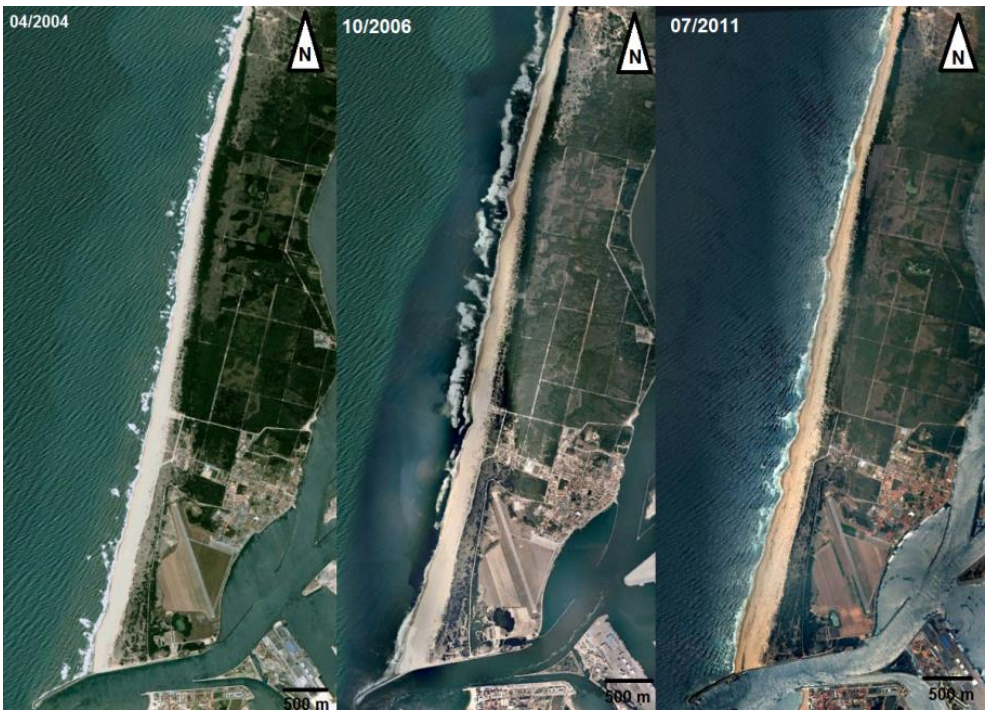

Figure 2 - Recent evolution of S. Jacinto beach and the sand cusps along the coastline (edited by GoogleEarth)

The northern Aveiro breakwater has been extended over the last decades due to navigation requirements at the inlet. Therefore, the beach has been increasing in width due to sediment accretion. The mean sediment diameter is around 0.2 mm determined with a simple optical analysis. S. Jacinto can be characterized by a barred beach during the maritime winter and by a low tide bar or rip beach during the

maritime summer according to the beach classification proposed by Masselink and Short (1993). This classification takes into account the wave height at breaking, the mean tidal range, the wave period and the sediment fall velocity. Therefore, the shift between winter and summer seasons demonstrates the large morphodynamic variability of S. Jacinto beach around its equilibrium profile.

The field campaign took place on 18 June 2015 during one tidal cycle. During this period and based on the Viana do Castelo meteorological station operated by IH, the atmospheric pressure remained constant (1020 hPa, MSL), the wind speed was weak during the morning (approx. 1 m/s) and increased for the rest of the day (up to 7.5 m/s). The tidal range measured at the tidal gauge located at Aveiro southern jetty was 2 m. The wave events results from the succession of 13 s to 10 s swell from NW. During the tidal cycle, Hs varied between 1.2 and 1.8 m. The associated swell Tp was higher in the morning (13 s) and vanished during the afternoon (10 s). Moreover, the wind increase leads to the development of seas (6 s) in the wave spectrum. The mean wave direction did not change around the most frequent NWW direction.

2.2 Description of the field campaign

The equipment deployed in the field campaign were an acoustic Doppler current profile (ADCP), two acoustic vector averaging current meters (SC), eight pressure transducers (PT) and two acoustic Doppler velocimeters (ADV) (Figure 3). The ADCP was moored at 11 m depth (HZ) to obtain the wave parameters before depth-induced transformations. Both SC were used to estimate the horizontal current profile near the bottom (0.5 m) just before the waves started to shoal. Further toward the beach, an array of eight pressure transducers were deployed perpendicular to the coastline in order to measure the wave shoaling and breaking during all the tidal cycle. Two ADV were mounted on a steel structure to measure the currents in the inter-tidal zone.

Figure 3 - Locations of the equipment deployed during the field campaign in S. Jacinto beach at high-water (edited by GoogleEarth)

Between the breaker zone and the coastline, a complex system of tidal and wave currents constantly shapes the beach profile. However, measuring such a chaotic environment has been presenting some limitations. Therefore, several drifters were launched by a jet ski seawards of the breaking zone in order to obtain the chaotic current pattern at the surface (Figure 4). Bathymetry was measured at the seaward side of the breaking zone by boat, up to 7 m (TR), and topographic survey carried out during low water and high water by a quad bike, from -1 m (TR). In the shadow zone between the two surveyed areas was the

water elevation of the several PT was adjusted to the curve of the tidal gauge. In this way, it was possible to attempt a production of the topo-bathymetry of S. Jacinto beach.

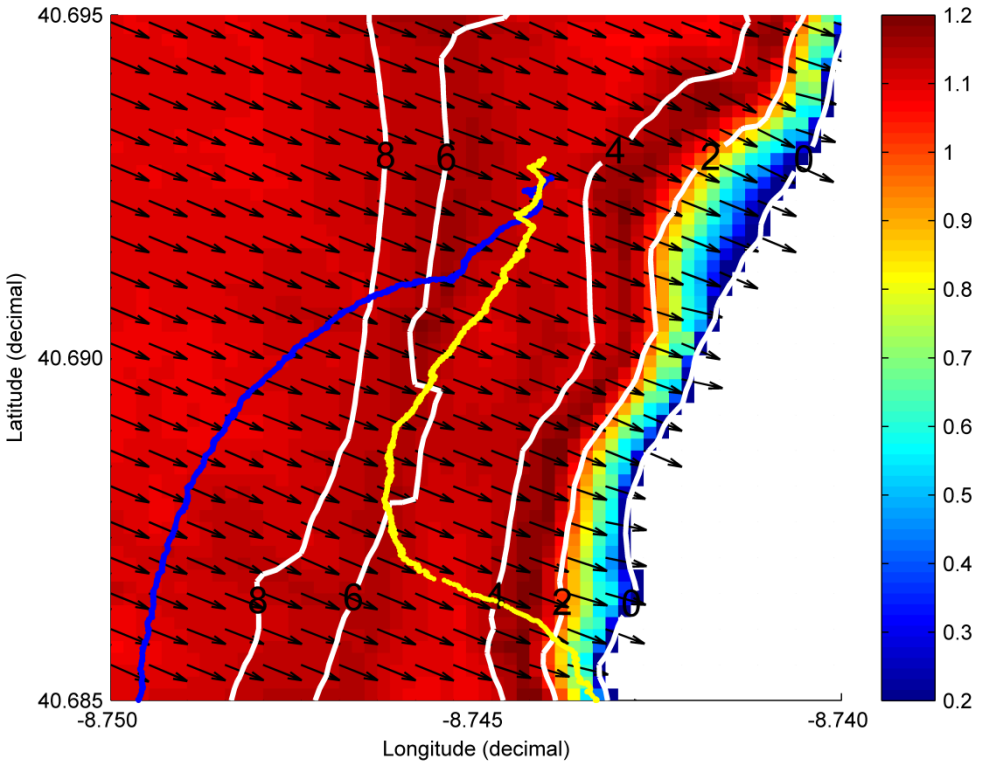

Figure 4 - Drifters trajectories due to the current at the sea surface (blue and yellow lines), water depth contours (white lines in m), Hs (m) obtained by the numerical model and the wave direction (arrows)

2.3 Setup of the equipment to measure wave parameters

The ADCP measured with a sampling interval of 2 Hz for the wave orbital velocities, the pressure of the water column and the distance to the water surface with sonar. We obtained three wave spectra with a Fourier transform to assess the accuracy of this instrument. After the spectra integration we were able to obtain the wave parameters (Hs, Tp, Dir, peak wave direction (PDir) and wavelength). Both SC measured the pressure of the water column with a sampling frequency of 0.5 Hz which was converted in water elevation. The water elevation was converted to spectra with a Fourier transform and the further integration allowed us to obtain the Hs and Tp. The PT measured the pressure at a sample frequency of 2 Hz and the methodology followed to obtain Hs and Tp was similar to the SC. All the previous equipment were transported to the breaking zone by boat and were deployed at the sea bottom by divers. Before the field campaign the equipment was calibrated for pressure in laboratory and did not display significant differences regarding the calibration curve. Finally, the PT were attached to concrete weights and deployed at the sea bottom with an average distance of 30 m between them. This arrangement of pressure sensors moorings allowed the measurement of the wave parameters in the near-shore area.

3. Methodology to modelling near-shore areas

The numerical model currently in development at Instituto Hidrográfico aims to simulate the wave and current interaction in coastal areas. The final objective is to make it an operational model. For that reason, the wave model relies on the mild-slope equation which simulates the wave diffraction and refraction

(Equation 1). However, previous formulation is usually solved for the complex amplitude which significantly increases the computational time because the model needs ten points per wavelength for accurate results. Here, we change the previous formulation by using the Eikonal form. This way, two equations were obtained: mass conservation for the wave action (Equation 2) and momentum equation for the wave number (Equation 3). With the previous formulation, the model gives accurate results for academic test cases (not shown here) with only four points per wavelength. Therefore, the computational cost was reduced and the simulations took, in average, 180 s in a laptop with an Intel Core(TM) i5-2430M with 2.4 GHz.

$$\nabla\left(CC_g\nabla\psi\right) + k^2 CC_g\nabla\psi = 0 \tag{1}$$

$$\frac{\partial N}{\partial t} + \nabla\cdot\left(\frac{CC_g}{\omega}\boldsymbol{k}N\right) = 0 \tag{2}$$

$$\frac{\partial \boldsymbol{k}}{\partial t} + \left(\frac{CC_g}{\omega}\boldsymbol{k}\cdot\nabla\right)\boldsymbol{k} + \frac{\partial\omega}{\partial h}\nabla h - \frac{CC_g}{2\omega}\nabla Y = 0 \tag{3}$$

where ∇ is the horizontal gradient operator [$\nabla = (\partial/\partial x, \partial/\partial y)$], C is the phase velocity, C_g is the group velocity, k is the wave number, ψ is the complex velocity potential, N is the wave action, ω is the wave frequency, $\boldsymbol{k}$ is the wave number vector, h is the bottom depth and Y are the terms related to wave diffraction and to the vertical structure in such a way that [$k^2 = k_0^2 + Y$] is satisfied and the wave number is obtained through the dispersion relationship [$\omega^2 = g\, k_0 \tanh(k_0 h)$].

4. Preliminary results

The bathymetry used in the numerical model was obtained during the field campaign as mentioned in Section 2. The model was run for two different conditions, during the flood and the ebb. Those were the tidal phases where the current was weaker and the results of the wave model would be least corrupted due to wave-current interaction. The input wave parameters at the boundaries were obtained by the ADCP (Table 1). The bottom dissipation mechanism and the wave dissipation through wave breaking were taken into account.

Table 1 – Tide and wave initial conditions for the wave model

Tide	Water level (m)	Hs (m)	Tp (s)	PDir (º)
Flood – 14h40	3.08	1.21	11.6	296
Ebb – 22h20	0.91	0.98	11.3	294

Results show a very good agreement between the model and the observations for the two selected situations (Figure 5). During the flood (red lines and circles), the model reproduced a shoaling of 10 cm against the 13 cm in data between the most offshore PT. Next, the model dropped 10 cm due to wave breaking while the fall in data was 20 cm. During the ebb, the model could simulate very well the peak of the wave shoaling revealed by the data. However, the dissipation was not accurately simulated by the wave model because the fall was only of 10 cm against the 20 cm in the data. The wave parameters recorded by the PT show the wave shoaling and further dissipation. Previous dissipation seems to extend until the shoreline which would enhance the long-shore currents. This evidence also suggests the importance of widening the dissipation along the breaking zone. Overall, such a simple model could reproduce the wave qualitative behaviour very well along a cross-shore profile.

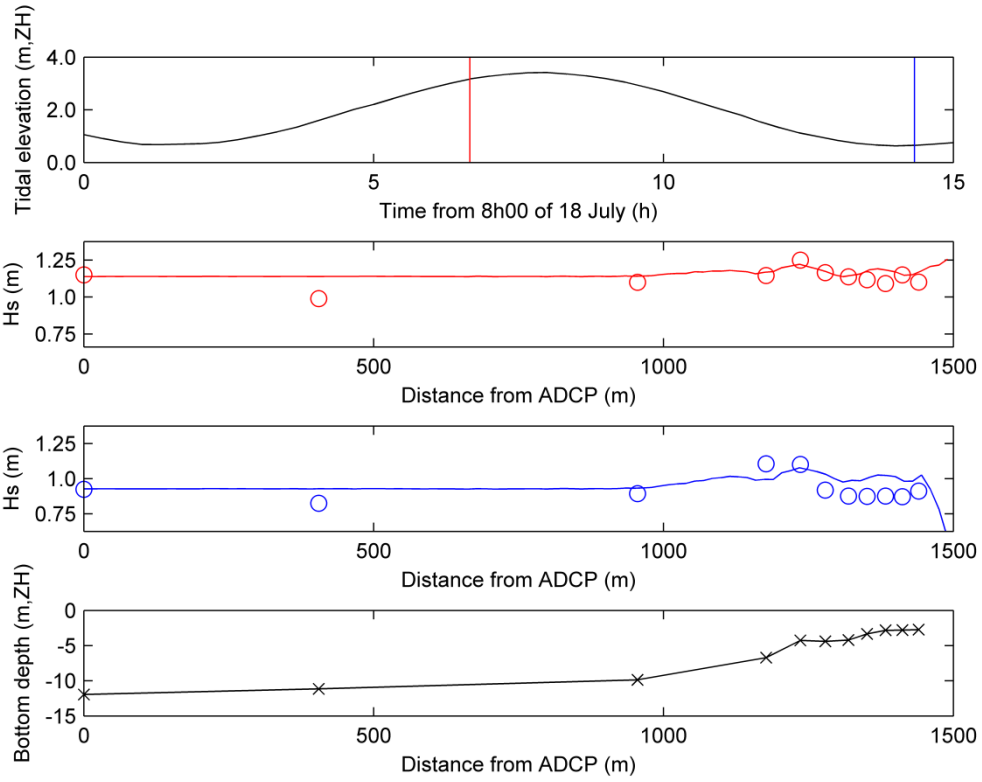

Figure 5 - Time series of the tidal curve obtained by the ADCP (first panel), Hs data (circles) and model (lines) along the array during the flood (red) and during the ebb (blue) (second and third panels) and bottom depth obtained from the equipment deployed (fourth panel)

5. Conclusions

In spite of the complex interactions between waves and currents in the near-shore zone, we achieved our primary goal of measuring wave parameters in the breaking zone. However, a serious limitation was imposed by the lack of bathymetric data in the breaking zone, which calls for a major improvement in our ability to conduct topo-bathymetric surveys in of the near-shore areas in future campaigns. Regarding the second objective, the numerical model application and based on our preliminary results, the model was able to reproduce the wave shoaling and dissipation.

Acknowledgments

Thanks are due to all the people that contributed and participated in the field campaign. This research is a contribution to project RAIA.CO(0520_RAIA_CO_1_E), *Observatório Marinho da Margem Ibérica e Litoral*, funded by the European Fund for Regional Development (EFDR) through the *Programa Operacional de Cooperação Transfonteiriça Espanha-Portugal* (POCTEC).

References

Austin, M. J., Scott, T. M., Russell, P. E., & Masselink, G. (2012). Rip current prediction: development, validation, and evaluation of an operational tool. Journal of coastal research, Vol. 29, No. 2, Págs. 283-300.

Berkhoff, J. C. W., Booy, N., & Radder, A. C. (1982). Verification of numerical wave propagation models for simple harmonic linear water waves. Coastal Engineering, Vol. 6, No. 3, Págs. 255-279.

Birkemeier, W. A., Long, C. E., & Hathaway, K. K. (1996). DELILAH, DUCK94 & SandyDuck: Three nearshore field experiments. Coastal Engineering Proceedings, Vol. 1, No. 25.

Booij, N., Ris, R. C., & Holthuijsen, L. H. (1999). A third-generation wave model for coastal regions: 1. Model description and validation. Journal of Geophysical Research: Oceans (1978–2012), Vol. 104 No. C4, Págs. 7649-7666.

Chassignet, E. P., Hurlburt, H. E., Smedstad, O. M., Halliwell, G. R., Hogan, P. J., Wallcraft, A. J., Bleck, R. (2007). The HYCOM (hybrid coordinate ocean model) data assimilative system. Journal of Marine Systems, Vol. 65, No. 1, Págs. 60-83.

Dingemans, M. W. (1997). Water wave propagation over uneven bottoms: Linear wave propagation (Vol. 13). World Scientific.

Lim, H. S., Chun, I. S., Kim, C. S., Park, K. S., Shim, J. S., & Yoon, J. J. (2013, March). High-resolution operational coastal modeling system for the prediction of hydrodynamics in Korea using a wave-current coupled model. In D. C. Conley, G. Masselink, P. E. Russell, & T. J. O'Hare (Eds.), Proceedings 12th International Coastal Symposium, Págs. 314-319.

Masselink, G., & Short, A. D. (1993). The effect of tide range on beach morphodynamics and morphology: a conceptual beach model. Journal of Coastal Research, Págs. 785-800.

Sharma, A., Panchang, V. G., & Kaihatu, J. M. (2014). Modeling nonlinear wave–wave interactions with the elliptic mild slope equation. Applied Ocean Research, Vol. 48, Págs. 114-125.

Shi, F., Kirby, J. T., Harris, J. C., Geiman, J. D., & Grilli, S. T. (2012). A high-order adaptive time-stepping TVD solver for Boussinesq modeling of breaking waves and coastal inundation. Ocean Modelling, Vol. 43, Págs. 36-51.

Tolman, H. L. (2002). User manual and system documentation of {WAVEWATCH-III} version 2.22.